Thermodynamics of Sodium Dodecyl Sulfate Partitioning into Lipid Membranes

Anmin Tan, André Ziegler, Bernhard Steinbauer, and Joachim Seelig
Department of Biophysical Chemistry, Biozentrum, University of Basel, CH-4056 Basel, Switzerland

ABSTRACT The partition equilibria of sodium dodecyl sulfate (SDS) and lithium dodecyl sulfate between water and bilayer membranes were investigated with isothermal titration calorimetry and spectroscopic methods (light scattering, ^{31}P-nuclear magnetic resonance) in the temperature range of 28°C to 56°C. The partitioning of the dodecyl sulfate anion (DS^-) into the bilayer membrane is energetically favored by an exothermic partition enthalpy of $\Delta H_D^0 = -6.0$ kcal/mol at 28°C. This is in contrast to nonionic detergents where ΔH_D^0 is usually positive. The partition enthalpy decreases linearly with increasing temperature and the molar heat capacity is $\Delta C_p^0 = -50 \pm 3$ cal mol^{-1} K^{-1}. The partition isotherm is nonlinear if the bound detergent is plotted versus the free detergent concentration in bulk solution. This is caused by the electrostatic repulsion between the DS^- ions inserted into the membrane and those free in solution near the membrane surface. The surface concentration of DS^- immediately above the plane of binding was hence calculated with the Gouy-Chapman theory, and a strictly linear relationship was obtained between the surface concentration and the extent of DS^- partitioning. The surface partition constant K describes the chemical equilibrium in the absence of electrostatic effects. For the SDS-membrane equilibrium K was found to be 1.2×10^4 M^{-1} to 6×10^4 M^{-1} for the various systems and conditions investigated, very similar to data available for nonionic detergents of the same chain length. The membrane-micelle phase diagram was also studied. Complete membrane solubilization requires a ratio of 2.2 mol SDS bound per mole of total lipid at 56°C. The corresponding equilibrium concentration of SDS free in solution is $C_{D,f}^{sol} \sim 1.7$ mM and is slightly below the critical micelles concentration (CMC) = 2.1 mM (at 56°C and 0.11 M buffer). Membrane saturation occurs at ~ 0.3 mol SDS per mol lipid and the equilibrium SDS concentration is $C_{D,f}^{sat} \approx 2.2$ mM $\pm$ 0.6 mM. SDS translocation across the bilayer is slow at ambient temperature but increases at high temperatures.

INTRODUCTION

Sodium dodecyl sulfate (SDS) is a commonly used detergent to solubilize biological membranes and to isolate and purify membrane proteins and membrane lipids. The critical micellar concentration (CMC) of SDS has been determined as early as 1959 (Mysels and Princen, 1959), and the SDS micellization behavior has been characterized in detail (Majhi and Blume, 2001; Chatterjee et al., 2001). In contrast, the interaction of SDS with lipid membranes is ill-described as far as the thermodynamics of this partition equilibrium is concerned. Using equilibrium dialysis Kragh-Hansen et al. (1998) report a partition constant of SDS for lipid model membranes and sarcoplasmic reticulum membranes of ~ 6000 M/M (moles detergent per liter lipid phase divided by moles detergent per liter aqueous phase), a saturating concentration of SDS of 0.9 mM, and a corresponding binding limit of 1.8 mol detergent taken up per mole phospholipid. Although this information seems sufficient for biochemical applications it does not provide an adequate thermodynamic description of the binding process. In fact, no thermodynamic description of the SDS water-membrane equilibrium appears to be available. Binding of SDS is favored by the hydrophobic adhesion of the hydrocarbon chains but is impeded by electrostatic repulsion of the negatively charged head groups. The insertion of SDS molecules into an electrically neutral lipid membrane produces a negative surface charge repelling, in turn, other SDS molecules near the membrane surface. The adsorption of SDS molecules will thus become increasingly more difficult as the membrane is loaded with dodecyl sulfate anions. Experimental evidence for an SDS-induced membrane surface charge was obtained in competition experiments with vesicles containing the anionic fluorescent probe 2-(*p*-toluidinyl) naphthalene-6-sodium sulfonate (Cocera et al., 2000). Upon binding of SDS, the probe was expelled from the membrane, and the fluorescence decreased. The change in fluorescence intensity was used to construct a binding isotherm. Electrostatic effects on SDS itself were, however, not considered and the binding constant varied considerably with the SDS concentration used.

We have measured the SDS water-membrane partition equilibrium for different types of model membranes with high sensitivity isothermal titration calorimetry (ITC). The insertion of the dodecyl sulfate anion into the membrane is associated with a distinct exothermic reaction and binding isotherms could be measured conveniently between 5 μM and 3 mM total SDS concentration. Electrostatic interactions were taken into account by calculating the SDS surface concentration by means of the Gouy-Chapman theory. The binding isotherms were analyzed in terms of a surface partition model corrected for electrostatic repulsion. We

Received for publication March 15, 2002, and in final form May 24, 2002.
Address reprint requests to Joachim Seelig, Department of Biophysical Chemistry, Biozentrum, University of Basel, Klingelbergstrasse 70, CH-4056 Basel, Switzerland. Tel.: 41-61-267-2190; Fax: 41-61-267-2189; E-mail: joachim.seelig@unibas.ch.

0006-3495/02/09/1547/10 $2.00

have furthermore used light scattering and phosphorus nuclear magnetic resonance to monitor the phase boundaries of the SDS water-membrane partition equilibrium at SDS saturation and solubilization conditions.

MATERIALS AND METHODS

Materials

1-Palmitoyl-2-oleoyl-*sn*-glycero-3-phosphocholine (POPC) and 1-palmitoyl-2-oleoyl-*sn*-glycero-3-phosphoglycerol (POPG) were purchased from Avanti Polar Lipids (Alabaster, AL). SDS and lithium dodecyl sulfate (LiDS) were from Bio-Rad Laboratories (Hercules, CA), and from Fluka (Buchs, Switzerland), respectively. All other chemicals were of analytical or reagent grade. Buffer was prepared from 18 MΩ water obtained from a NANOpure A filtration system.

Preparation of vesicles

A defined amount of lipid in chloroform was first dried under nitrogen. The lipid was dissolved in dichloromethane, again dried under nitrogen and, subsequently, overnight under high vacuum. Typically, 2 to 3 mL of buffer (10 mM Tris, 100 mM NaCl, pH 7.4) were added to the lipid, and the dispersion was extensively vortexed. Small unilamellar vesicles (SUV) with an average diameter of 30 nm were prepared by sonication in ice water using a titanium-tip ultrasonicator (10–15 min) until the solution became transparent. Titanium debris was removed by centrifugation (Eppendorf tabletop centrifuge, 10 min at 16,000 × *g*).

Large unilamellar vesicles (LUV) with a diameter of 100 nm were prepared by extrusion using polycarbonate filters with 100-nm pore size (MacDonald et al., 1991).

For the nuclear magnetic resonance (NMR) measurements mixtures of SDS and POPC were prepared in 8-mm (outer diameter) test tubes. A defined amount of lipid in dichloromethane was first dried under nitrogen and subsequently under high vacuum. The dry lipid was weighed, and the appropriate volume of an SDS solution was added to achieve the desired molar ratio. The dispersions were gently vortexed until a homogeneous preparation was obtained. The lipid concentration was between 10 and 20 mM.

Calorimetry

Isothermal titration calorimetry was performed using a MicroCal VP high-sensitivity titration calorimeter (MicroCal, Northampton, MA) (Wiseman et al., 1989). To avoid air bubbles, the solutions were degassed under vacuum prior to use. The data were acquired by computer software developed by MicroCal.

NMR measurements

Solid-state ^{31}P-NMR measurements were performed with a Bruker AMX 400 spectrometer operating at 161 MHz. A spin echo sequence with gated proton decoupling was used. The $\pi/2$ pulse width was 3 μs, the interpulse spacing was 40 μs, and the recycling delay 5 s. One thousand free induction decays were accumulated and processed with a 100-Hz line broadening prior to Fourier transformation.

Right-angle light scattering

Light-scattering measurements were made with a Jasco FP 777 spectrofluorimeter (Japan-Spectroscopic, Tokyo, Japan) with the excitation wavelength set at 350 nm. The optical cuvette with 3 mL of the detergent solution was thermostatted at a defined temperature and was continuously stirred. Vesicles (C_L = 26 mM, 100-nm diameter) were added in 10 μL aliquots using a Hamilton syringe. The scattering intensity was recorded as a function of time and evaluated at 350 nm. As a control lipid, vesicles were injected into buffer without SDS.

Binding model

Different models have been proposed to describe the partitioning of a surfactant between a membrane and the aqueous phase (Lasch, 1995). According to our experience, the best model for *nonionic* detergent-membrane systems is a simple partition equilibrium of the form (Schurtenberger et al., 1985)

$$R_b = KC_{D,f} \tag{1}$$

in which $R_b = C_{D,b} / C_L^0$ is the molar ratio of bound surfactant to total lipid and $C_{D,f}$ is the equilibrium concentration of surfactant free in solution (Heerklotz and Seelig, 2000b; Wenk et al., 1997; Wenk and Seelig, 1997). For a *charged* surfactant such as SDS, Eq. 1 must be modified since the binding of SDS imparts a negative surface charge σ and a negative surface potential ψ_0 to the membrane. In equilibrium, the surfactant concentration near the membrane surface, $C_{D,S}$, is smaller than the bulk concentration according to Boltzmann's law:

$$C_{D,S} = C_{D,f} \times e^{-zF_0\psi_0/RT} \tag{2}$$

in which z denotes the signed charge of the detergent, F_0 is the Faraday constant, and RT is the thermal energy. For SDS binding, Eq. 1 must thus be replaced by

$$R_b = KC_{D,s} = K \times C_{D,f} \times e^{-zF_0\psi_0/RT} \tag{3}$$

The membrane surface charge density σ can be calculated from R_b:

$$\sigma = \frac{e_0}{A_L} \frac{R_b}{1 + R_b(A_D/A_L)} \tag{4}$$

e_0 is the signed charge of an electron, A_L is the cross sectional area of a phospholipid (POPC, 68 × 10^{-20} m^2) (Altenbach and Seelig, 1984), and A_D is the cross-sectional area of SDS in the membrane (~30 × 10^{-20} m^2). Eq. 4 includes the expansion of the membrane surface due to the insertion of SDS between the lipid molecules. Knowledge of the membrane surface charge density allows the calculation of the membrane surface potential ψ_0 using the Gouy-Chapman theory (Aveyard and Haydon, 1973; McLaughlin, 1977)

$$\sigma^2 = 2000\varepsilon_0\varepsilon_r RT \sum_i C_{i,eq}(e^{-z_i F_0\psi_0/RT} - 1) \tag{5}$$

in which ε_r is the temperature-dependent dielectric constant of water, ε_0 is the permittivity of free space, $C_{i,eq}$ the concentration of the ith electrolyte in the bulk aqueous phase (in molars), and z_i the signed valency of the ith species. In the present study R_b was measured with isothermal titration calorimetry and σ was then determined with Eq. 4. Finally a computer program was used to numerically evaluate ψ_0, and the binding constant K by searching for K, ψ_0-pairs, which simultaneously fulfill Eqs. 3 to 5.

Measurements were also made with negatively charged vesicles composed of POPC/POPG (3:1 molar ratio). POPG not only confers a negative charge to the membrane surface but also binds Na^+ ions with a binding constant of K_{Na+} = 0.6 M^{-1}. The binding follows a Langmuir adsorption isotherm, modified again for electrostatic effects (Nebel et al., 1997).

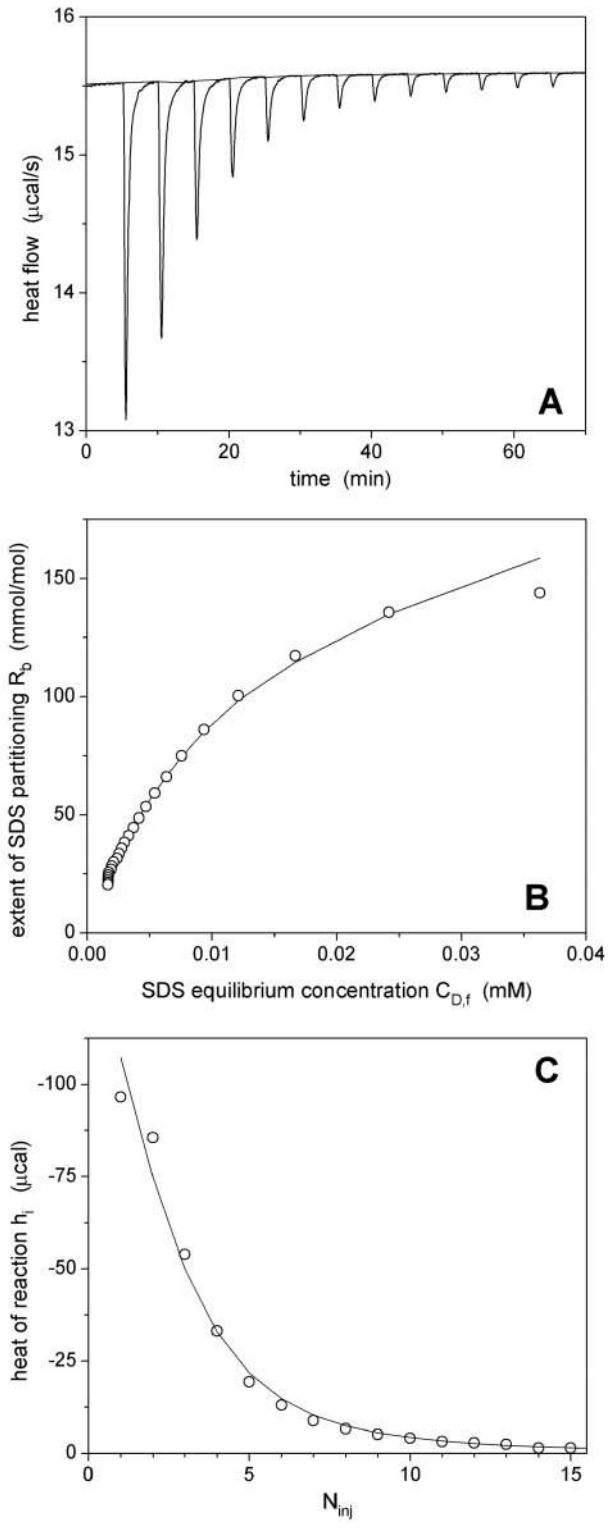

FIGURE 1 Lipid-into-SDS titration. (*A*) Titration calorimetry of SDS (50 μM) with 100-nm unilamellar POPC vesicles (26.3 mM) in buffer (10 mM Tris, 100 mM NaCl, pH 7.4, 28°C). Each peak corresponds to the addition of 10-μL vesicle suspension to the SDS solution in the calorimeter cell (cell volume 1.4037 mL). (*B*) Binding isotherm for SDS partitioning into POPC vesicles. The extent of binding R_b (the molar amount of SDS bound per mole lipid) is plotted against the equilibrium concentration, $C_{D,f}$, of detergent free in solution. (○) Experimental results derived from *A*. The solid line is the theoretical analysis using Eqs. 2 to 4. (*C*) The heat of reactions, h_i, as a function of the injection number N_{inj}. Experimental results (○) compared with theory (*solid line*). The theoretical analysis in *B* and *C* is based on a partition constant of $K = 2.3 \times 10^4\ M^{-1}$ and $\Delta H_D^0 = -5.1$ kcal/mol. Only the lipid in the outer half-layer was considered to be available for SDS binding (50% of total lipid).

RESULTS

Binding isotherms measured with isothermal titration calorimetry

Fig. 1 *A* displays the titration of SDS ($C_D^0 = 50\ \mu$M in buffer) with large unilamellar POPC vesicles ($C_L^0 = 26.3$ mM) at 28°C. Each 10 μL injection gives rise to an exothermic heat of reaction, h_i, produced by the partitioning of dodecyl sulfate anion (DS^-) into the membrane; h_i is given by the area of the titration peak. With consecutive injections h_i decreases in magnitude as the free detergent is gradually adsorbed by lipid. Baseline values are reached after ~ 10 injections and almost all SDS is bound to lipid. The molar heat of reaction is

$$\Delta H_D^0 = \sum_{i=1}^{10} h_i \Big/ (C_D^0 \cdot V_{cell}) = -5.1 \text{ kcal/mol}$$

($V_{cell} = 1.4037$ mL is the volume of the calorimeter cell). The corresponding extent of binding, $R_b^{(i)}$, after *i* injections is calculated as

$$R_b^{(i)} = \sum_{1}^{i} h_k/(\Delta H_D^0 \times C_D^0 \times V_{cell}) \quad (6)$$

The equilibrium concentration of SDS remaining free in solution, $C_{D,f}$, is then obtained as the difference between the total SDS in the calorimeter cell and that bound to the injected lipid.

$$C_{D,f}^{(i)} = C_D^0 - R_b^{(i)} C_L^{(i)} \quad (7)$$

The variation of R_b with $C_{D,f}$ is shown in Fig. 1 *B*. The calculation of the binding isotherm is based on the lipid of the outer half-layer only (LUVs, 50% of total lipid; SUVs, 60% of total lipid). As the SDS molecule is charged, a translocation to the inner halflayer is hindered at low concentrations of SDS and low temperatures. The open circles in Fig. 1 *B* represent the true binding isotherm as derived from the calorimetric measurement without assuming a specific binding model, the solid line is the theoretical analysis. The figure reveals a nonlinear dependence of R_b on the equilibrium concentration, $C_{D,f}$. If an apparent binding constant is defined according to Eq. 1, it will vary with $C_{D,f}$. Typical values for K_{app} as deduced from Fig. 1 *B* are $K_{app} = 1.1 \times 10^4\ M^{-1}$ and $4.5 \times 10^3\ M^{-1}$ at concentrations of 2 μM and 25 μM, respectively. In contrast, the theoretical line was calculated with a single binding constant of $K =$

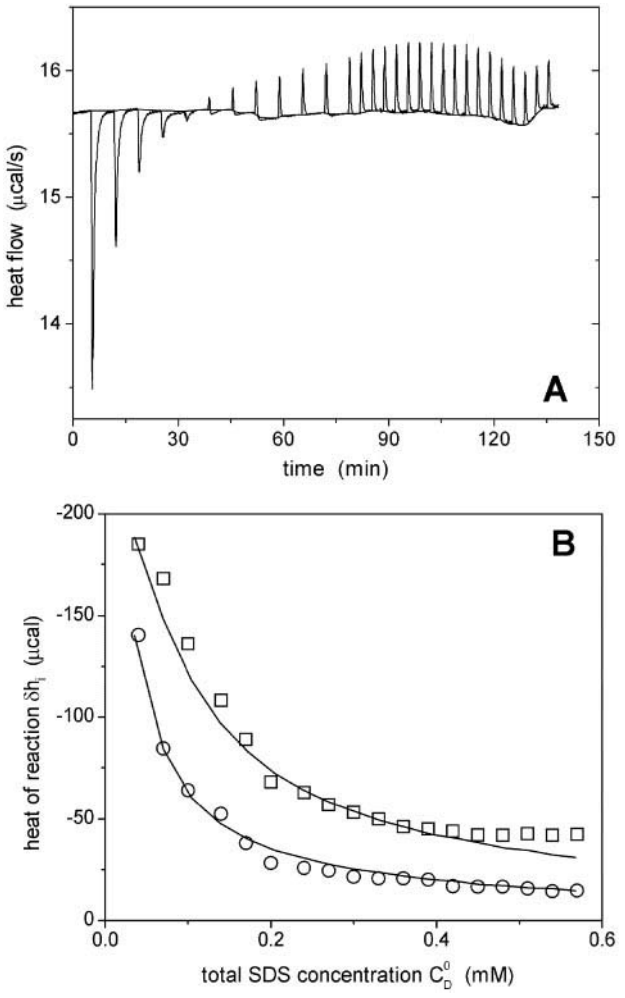

FIGURE 2 SDS-into-lipid titration. (*A*) The calorimeter cell (V_{cell} = 1.4037 mL) contained large unilamellar POPC vesicles (100 nm) at a concentration of C_L^0 = 0.5 mM, which were titrated with a C_D^0 = 5 mM SDS solution. Each titration peak corresponds to a 10-μL injection of SDS solution. Measuring temperature 28°C. (*B*) Corrected heats of titration, h_i, as a function of the total SDS concentration in the calorimeter cell. (○) C_L^0 = 0.5 mM. (□) C_L^0 = 1.0 mM. The solid lines were calculated with a partition constant $K = 1.5 \times 10^4$ M^{-1} and a reaction enthalpy of $\Delta H_D^0 = -4.8$ kcal/mol. The calculation was based on the lipid of the outer half-layer only (50% total lipid). At 28°C a translocation of SDS into the inner monolayer is kinetically hindered. The demicellization of SDS was measured in a separate experiment (SDS-into-buffer titration) and is h_i = 31 μcal for a 10-μL injection. This value was subtracted from all individual peaks of Fig. 2 *A*. In the SDS-into-POPC titration experiment the free SDS concentration even after 30 injections remains much below the CMC.

2.3×10^4 M^{-1}. Fig. 1 *C* finally shows the comparison between the measured reaction enthalpies, h_i, (open circles) and the theoretical prediction (solid line) using $K = 2.3 \times 10^4$ M^{-1} and $\Delta H_D^0 = -5.1$ kcal/mol.

The reverse titration experiment, i.e., the titration of lipid vesicles (in the calorimeter cell) with SDS (in the syringe) is shown in Fig. 2. The calorimeter cell contains phospholipid vesicles (diameter ~ 100 nm) at *low* lipid concentration (0.5 mM), which are titrated with a 5-mM SDS solution. The experimental conditions are closely related to those used by Cocera et al. (2000) in their dye competition experiment (Fig. 1). Two reactions take place simultaneously: 1) demicellization of SDS and 2) binding of SDS to the outer lipid layer. The critical micellar concentration of SDS is 1.57 mM under the present conditions (28°C; 0.1 M NaCl, 10 mM Tris, pH 7.4; measured with ITC), which is in agreement with Paula et al. (1995). Injection of 10 μL of a 5 mM SDS solution into the calorimeter cell (V_{cell} = 1.4037 mL) leads to a 140-fold dilution of the SDS concentration, and the SDS micelles disintegrate. The heat of demicellization was determined in a separate experiment by injecting the SDS solution into buffer without phospholipid. Demicellization is endothermic with a reaction enthalpy of $\Delta H_{demic}^0 = 0.8$ kcal/mol. In contrast, SDS binding to phospholipid vesicles is exothermic. Fig. 2 *A* demonstrates that the exothermic binding of SDS initially exceeds the endothermic demicellization reaction. However, after five injections the observed heats of reaction become endothermic and the demicellization reaction is now the heat-determining process. The heat of demicellization was then subtracted from the primary experimental data shown in Fig. 2 *A*. Fig. 2 *B* displays the variation of the corrected heats of DS^- insertion as a function of the total SDS concentration, C_D^0, for two different lipid concentrations (0.5 mM and 1 mM). The titration curves have the same shape as the fluorescence quenching experiments (Cocera et al., 2000, 2001). An initial strong binding is followed by a long tailing-off of the partition reaction. The solid lines represent the theoretical results calculated with the surface partition model. The same set of parameters ($K = 1.5 \times 10^4$ M^{-1}, $\Delta H_D^0 = -5.0$ kcal/mol) was used for both curves. These parameters are also very similar to those used for the lipid-into-SDS titration shown in Fig. 1.

Again the analysis was based on a binding of DS^- to the lipid outside only. The question of SDS flip-flop was not investigated in detail in the present study. Earlier fluorescent probe and radio label measurements concluded that the flip-flop rate of DS^- monomers across the lipid bilayer was very slow at 20°C (Cocera et al., 1999; Kragh-Hansen et al., 1998). For the evaluation of the ITC data half-sided binding was assumed for temperatures up to 40°C. At 50°C the lipid availability factor could be varied between 0.7 to 0.9. At 56°C the membrane dissolution experiments (discussed in the following section) indicated a 100% lipid availability, suggesting a rapid flip-flop of SDS across the membrane.

Table 1 summarizes the ITC data in numerical form. The ΔH^0 and C_p^0 values are deduced directly from the ITC measurements. The binding constants were evaluated using the Gouy-Chapman theory and describe the physical-chemical adsorption to the membrane free of electrostatic effects. Table 1 contains the thermodynamic data for 1) micelle formation, 2) partitioning of SDS into small (30 nm) and large (100 nm) unilamellar vesicles, 3) the temperature dependence of the binding reaction, 4) the binding of SDS

TABLE 1 Micelle formation*

Temp C	CMC M	ΔH^0_D kcal/mol	ΔG^0_D kcal/mol	$T\Delta S^0_D$ kcal/mol	$\Delta C^0_{p,D}$ cal mol^{-1} K^{-1}
28	1.57E − 03	−0.8	−6.3	5.5	
35	1.64E − 03	−1.5	−6.4	4.9	−91
40	1.78E − 03	−2.0	−6.4	4.4	
50	2.00E − 03	−2.8	−6.5	3.7	

SDS partitioning into lipid bilayers*

Temp C	K M^{-1}	ΔH^0_D kcal/mol	ΔG^0_D kcal/mol	$T\Delta S^0_D$ kcal/mol	$\Delta C^0_{p,D}$ cal mol^{-1} K^{-1}	c^0_{SDS} μM
SDS + POPC SUVs (30 nm)						
28	6.0E + 04	−5.9	−9.0	3.0		50
35	5.0E + 04	−6.2	−9.0	2.9	−54	50
40	4.0E + 04	−6.5	−9.1	2.6		50
50	3.0E + 04	−7.1	−9.2	2.1		50
SDS + POPC LUVs (100 nm)						
28	2.30E + 04	−5.1	−8.4	3.3		50
35	1.80E + 04	−5.4	−8.4	3.1	−48	50
40	1.60E + 04	−5.6	−8.5	2.9		50
50	1.25E + 04	−6.2	−8.6	2.5		50
SDS + POPC/POPG (3:1 mol/mol) SUVs (30 nm)†						
28	6.00E + 04	−6.0	−9.0	3.0		50
35	7.00E + 04	−6.3	−9.3	3.0	−65	50
40	6.00E + 04	−6.7	−9.3	2.6		50
50	4.50E + 04	−7.4	−9.4	2.0		50
LiDS + POPC SUVs (30 nm)						
28	4.00E + 04	−6.1	−8.7	2.6		50
35	3.50E + 04	−6.6	−8.8	2.2	−55	50
40	3.20E + 04	−6.8	−8.9	2.2		50
50	2.50E + 04	−7.4	−9.0	1.7		50
SDS + POPC SUVs (30 nm) as a function of the SDS concentration						
28	7.00E + 04	−5.5	−9.0	3.6		5
28	6.00E + 04	−5.6	−9.0	3.3		10
28	7.00E + 04	−5.6	−9.0	3.4		20
28	6.00E + 04	−5.9	−9.0	3.0		50
28	6.00E + 04	−7.1	−9.0	1.9		100

*All measurements in buffer (0.1 M NaCl, 10 mM Tris, pH 7.4).
†At 40 and 50°C a limited translocation of SDS across the bilayer is observed.

to negatively charged vesicles composed of POPG and POPC (PC/PG = 3/1), and 5) the binding of LiDS to POPC small unilamellar vesicles. LiDS is preferred for membrane protein purification at low temperature because it has a better solubility than SDS.

Membrane solubilization

As more and more SDS is added to the lipid bilayer, the membrane will first reach a point of saturation, R_b^{sat}, followed by complete solubilization at R_b^{sol}. $R_b^{sat} = C_D^{sat}/C_L^0$ describes the phase boundary between the pure bilayer phase and the bilayer/mixed micelle coexistence phase. The phase boundary between the bilayer/mixed micelle coexistence phase and the micellar phase is given by $R_b^{sol} = C_d^{sol}/C_L^0$.

We have studied vesicle solubilization with light scattering and ITC. For 90° light scattering the cuvette contained SDS solutions at concentrations between 1 and 3.5 mM to which 5 to 10 μL aliquots of POPC-LUVs (C_L^0 = 26 mM) were added. Fig. 3A shows the increase in scattering intensity as a function of the lipid concentration in the cuvette. For lipid vesicles injected into pure buffer or into 1 mM SDS at 28°C or 56°C, the scattering intensity increases linearly with the lipid concentration, no solubilization occurs. If the same experiment is repeated with 2 mM or 3 mM SDS solution at 28°C, the scattering intensity again increases initially but then decreases slowly over a period of 12 h or more. Apparently, the lipid bilayer is destroyed at these SDS concentrations but vesicle dissolution is a slow process at 28°C (compare Kragh-Hansen et al., 1998). In contrast, lipid injection into 2 mM or 3 mM SDS at 56°C leads to a clear solution within a few minutes, indicating a rapid solubilization of lipid vesicles. As more lipid is added, the free SDS concentration is reduced, and disintegration of

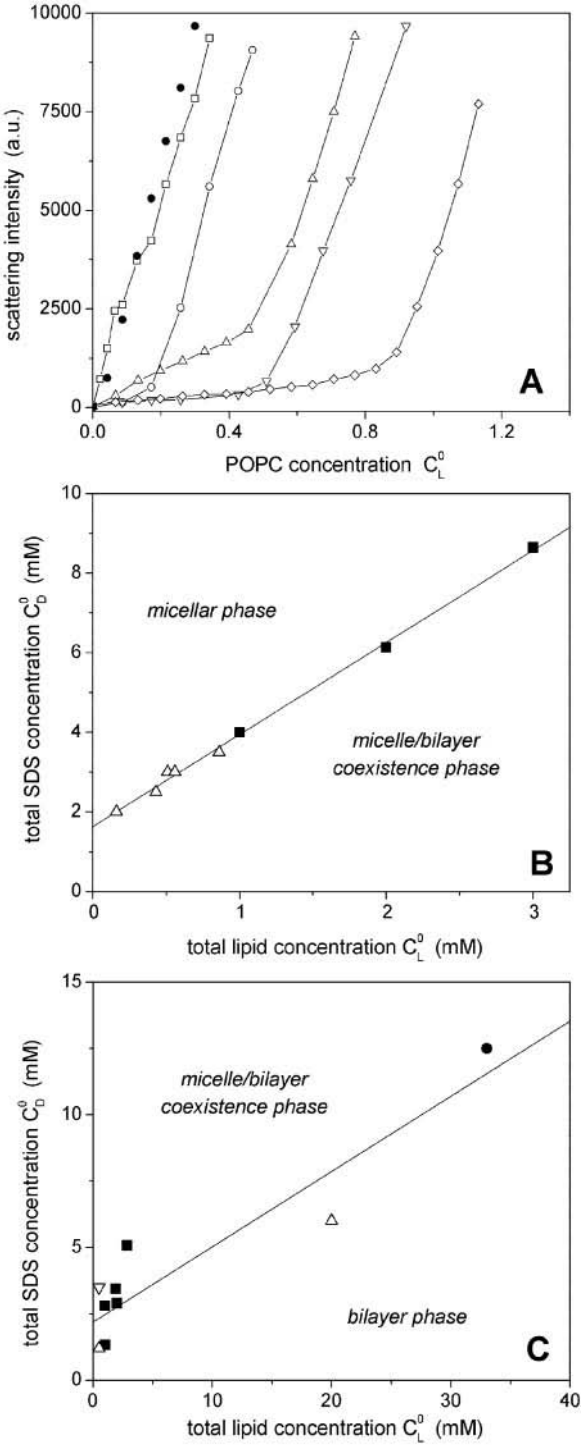

FIGURE 3 (*A*) 90° light scattering intensity as a function of phospholipid concentration as phospholipid vesicles are titrated into buffer or solutions of different SDS concentration. POPC LUVs (100 nm) were titrated into SDS solutions of different concentration. (●) Buffer, 56°C; (□) 1 mM SDS, 56°C; (○) 2 mM SDS, 56°C; (△) 2.5 mM SDS, 56°C; (▽) 3 mM SDS, 56°C; (◇) 3.5 mM SDS, 56°C. The concentration of the injected lipid stock solution was $C_L^0 = 26$ mM. Injection volumes 5 to 10 μL. Buffer, 10 mM Tris, 100 mM NaCl, pH 7.4. (*B*) Phase diagram of SDS-POPC at 56°C. Solubilization phase boundary between the bilayer micelles coexistence phase and the micellar phase. (*C*) Saturation boundary separating the bilayer phase from the bilayer/micelle coexistence region. (■) ITC at 56°C; (●) NMR at 56°C; (▽) light scattering data at 20°C (taken from Lopez et al. (1999)), (△) light scattering data at 56°C (this work).

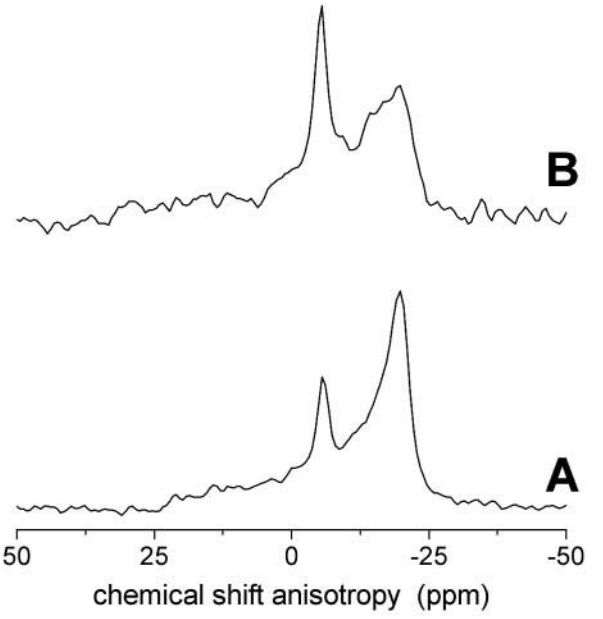

FIGURE 4 Phosphorus solid state NMR spectra of POPC membranes in mixtures with SDS at 6 mM. (*A*) Lipid concentration 20.3 mM. (*B*) Lipid concentration 12.3 mM.

LUVs comes to a halt. The scattering intensity then increases with the same slope as observed for the injection of lipid vesicles into pure buffer or 1 mM SDS at 56°C. Fig. 3 *A* shows that the scattering intensity starts to increase at $C_L^0 = 0.165$ mM (0.511 mM) if the detergent concentration is $C_D^0 = 2$ mM (3 mM). The light scattering data together with ITC experiments allow the construction of the phase boundary between the pure micellar phase and the bilayer/micelle coexistence phase. At the solubilization boundary the ratio of bound SDS-to-total lipid, $R_b^{sol} = C_D^{sol}/C_L^0$ is constant, and Eq. 7 can be rewritten (Almog et al., 1990; Lichtenberg et al., 1983)

$$C_D^0 = C_D^{sol} + R_b^{sol}\, C_L^0 \tag{8}$$

A plot of C_D^0 versus the corresponding C_L^0 at the phase boundary should yield a straight line with a slope of R_b^{sol} and an intersect C_D^{sol}. This is shown in Fig. 3 *B*. The boundary between pure micelles and the bilayer/micelle coexistence phase is given by (concentrations in mM):

$$C_D^0 = 1.69 + 2.2C_L^0 \tag{9}$$

Thus, the minimum SDS concentration to achieve complete solubilization at 56°C is $C_D^{sol} = (1.69 \pm 0.17)$ mM. The critical micellar concentration under the same conditions is

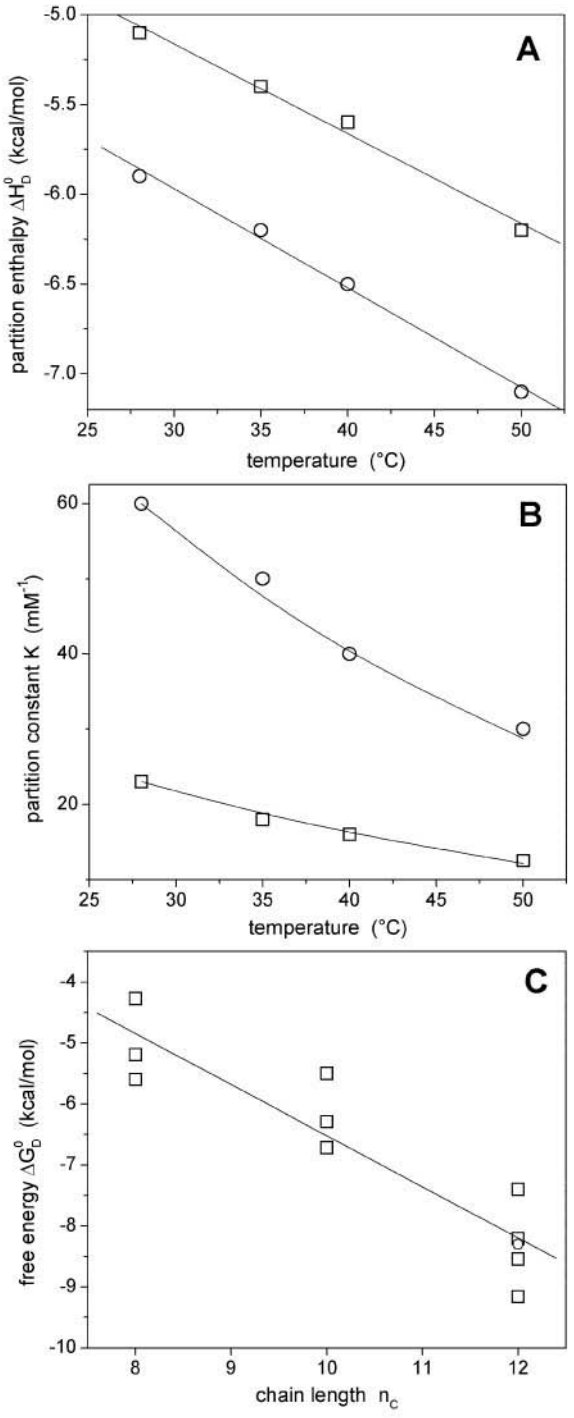

FIGURE 5 Partitioning of SDS into large and small unilamellar POPC vesicles. Temperature dependence of *A* the partition enthalpy ΔH_D^0, (*B*) the partition constant *K*. (○) SUVs (30 nm); (□) LUVs (100 nm). The solid lines in *B* show the theoretical temperature dependence of *K* as predicted from $d \ln K/dT = \Delta H_D^0/RT^2$ and $\Delta H_D^0(T) = \Delta H_D^0 + C_P(T - T_0)$ (Fig. 5 *A*). (*C*) The free energy, ΔG_D^0, of membrane partitioning for a variety of nonionic detergents is plotted against the hydrocarbon chain length and is compared with that of SDS. The experimental data for the nonionic detergents are taken from Heerklotz and Seelig (2000a) (Table 1). (□) Nonionic detergents; (○) SDS. The nonionic detergents included are (from bottom symbol to top symbol): C8, octyl-thioglucoside, -glucoside, -maltoside; C10, decyl-glucoside, $C_{10}EO_7$, decyl-maltoside; C12, $C_{12}EO_3$, $C_{12}EO_4$, $C_{12}EO_6$, dodecyl-maltoside.

2.1 mM. The detergent-to-lipid ratio at complete solubilization is $R_b^{sol} \approx 2.2 \pm 0.3$ mol SDS/mol lipid.

The phase boundary between the bilayer phase and the bilayer/micelle coexistence phase was determined with NMR and also with ITC. Fig. 4 displays phosphorus-31 NMR spectra of POPC bilayers in equilibrium with SDS at $C_D^0 = 6$ mM (at 56°C). Spectrum A ($C_L^0 = 20.3$ mM) is essentially a bilayer spectrum with a small contribution of an isotropic micellar phase. Decreasing the lipid concentration as in spectrum B ($C_L^0 = 12.3$ mM) increases the isotropic signal.

The phase boundary between the pure bilayer and the bilayer/micelle coexistence phase can also be determined by a plot of C_D^0 vs. C_L^0, selecting those C_D^0, C_L^0 pairs at which the bilayer shows the first sign of an isotropic signal. This phase boundary is shown in Fig. 3 *C*. The figure includes NMR, ITC, and light scattering data at 56°C, but also a previous light scattering result at 20°C (Lopez et al., 1998). The ITC data were obtained by titrating 1 to 3 mM lipid vesicle suspensions with 100 mM SDS solution. The regression analysis of all data yields

$$C_L^{sat} = 0.283 C_L^{sat} + 2.20 \quad (10)$$

The saturation limit of SDS in the membrane is $R_b^{sat} \approx 0.283 \pm 0.044$ and $C_D^{sat} \approx 2.20$ mM $\pm$ 0.6 mM. The scatter of the NMR data is larger than that observed in ITC measurements. Measurements at low lipid concentrations could only be made with ITC because the lipid concentration becomes very small for NMR, requiring prohibitively long NMR measuring times.

DISCUSSION

Partition enthalpy and molar heat capacity

Isothermal titration calorimetry provides the partition enthalpy, ΔH_D^0, the molar heat capacity, ΔC_p^0, and the partition isotherm, $R_b = f(C_{D,f})$, of the SDS water-membrane partition equilibrium. Fig. 5 shows the temperature dependence of the partition enthalpy, ΔH_D^0, for small (30 nm) and large (100 nm) unilamellar POPC vesicles. ΔH_D^0 decreases linearly with increasing temperature and the molar heat capacity for the transition from water to the membrane is $\Delta C_p^0 = -50 \pm 5$ cal mol^{-1} K^{-1} for all systems investigated (compare Table 1). The partition enthalpy is more negative for small than for large vesicles. This is a very general phenomenon that has been found for quite a variety of amphiphilic compounds with differences in ΔH of up to 20 kcal/mol (e.g., Beschiaschvili and Seelig, 1992; Gazzara et al., 1997) (compare below).

Two aspects are remarkable compared with nonionic detergents (Heerklotz and Seelig, 2000b): 1) SDS binding is exothermic and the partitioning into the membrane is thus energetically favorable. Nonionic and zwitterionic detergents and also free fatty acids (Richieri et al., 1995) exhibit unfavorable endothermic partition enthalpies at room temperature. Nonionic detergents typically have a bulky headgroup with a cross-sectional area larger than that of the hydrocarbon chains. In contrast, the SO_4^- headgroup of the DS^- anion is small, and steric repulsion at the headgroup level can be excluded. Hence, a tighter interaction of the DS^- hydrocarbon chain with the phospholipid fatty acyl chains could explain the exothermic ΔH_D^0 values. 2) The molar heat capacities of SDS and LiDS are smaller in magnitude than those of nonionic detergents. The large changes in the heat capacity of nonionic detergents are usually explained by a loss of hydration water around the hydrocarbon moieties as they enter the membrane (hydrophobic effect). For SDS this effect could be partially compensated by an increased hydration of the membrane surface, perhaps caused by the insertion of the polar sulfate group into the interface.

Equilibrium constant, *K*, and free energy, ΔG_D^0

The experimental titration isotherms reveal a nonlinear dependence between the amount membrane-bound surfactant, measured by R_b, and surfactant remaining free in solution, $C_{D,f}$ (compare Fig. 1 *B*). As the SDS concentration in the membrane increases, the partition isotherm is bent towards the *x* axis as a result of increased electrostatic repulsion between the membrane surface and the dodecyl sulfate anion. However, if the bulk concentration, $C_{D,f}$, is replaced by the surface concentration, $C_{D,S}$, a linear correlation between R_b and $C_{D,S}$ is predicted by Eq. 3. This is indeed borne out experimentally. Fig. 6 summarizes the analysis of the experimental data of Fig. 2 in terms of this model. Fig. 6 *A* shows the binding isotherm R_b vs. $C_{D,f}$ as deduced from Fig. 2, Fig. 6 *B* displays the same R_b values as a function of the surface concentration $C_{D,S}$, and Fig. 6 *C* shows the variation of the surface potential ψ_0. Inspection of Fig. 6 *B* reveals a linear relationship between bound surfactant, i.e., R_b, and the surface concentration, $C_{D,S}$, with the slope defining the partition constant *K* (Compare Eq. 3).

The temperature dependence of the SDS partition constant for POPC SUVs and LUVs is shown in Fig. 5 *B*. Because ΔH_D^0 is negative, the partition constant decreases with temperature. At high temperatures less SDS is incorporated into the lipid membrane. This is in contrast to the endothermic partitioning of nonionic detergents, which bind better at high temperatures.

The free energy of SDS partitioning can be calculated according to $\Delta G_D^0 = RT \ln(55.5\ \text{K})$ in which the factor 55.5 corrects for the cratic contribution (Cantor and Schimmel, 1980). Inspection of Table 1 reveals that ΔG_D^0 is of the order

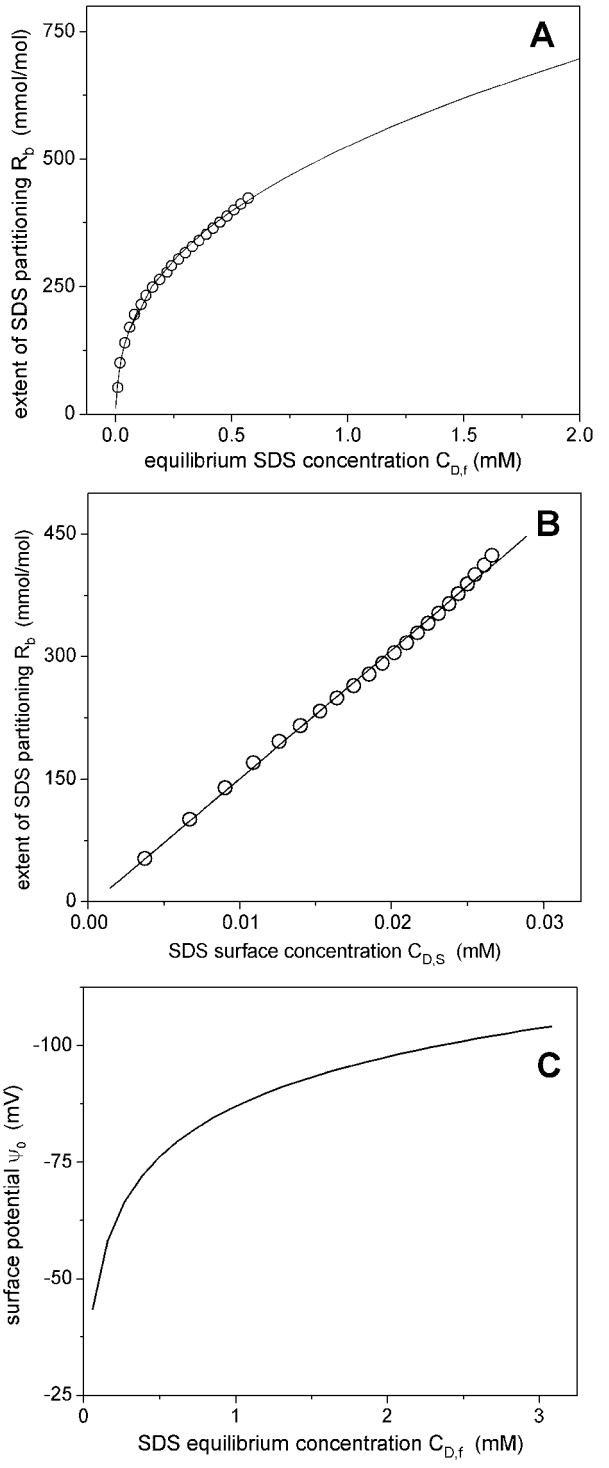

FIGURE 6 SDS partition isotherm and SDS-induced surface potential. (*A*) The extent of SDS binding $R_b = n_D^0/n_L^0$ as a function of the SDS equilibrium concentration, $C_{D,f}$. The open circles represent experimental data taken from Fig. 2 (injection of 5 mM SDS into a 1 mM POPC suspension). (*B*) R_b as a function of the SDS surface concentration, $C_{D,S}$ (calculated with the Gouy-Chapman theory). (*C*) Membrane surface potential, ψ_0, of POPC membranes as a function of the SDS equilibrium concentration, $C_{D,f}$. Only the outer half-layer was considered for SDS binding.

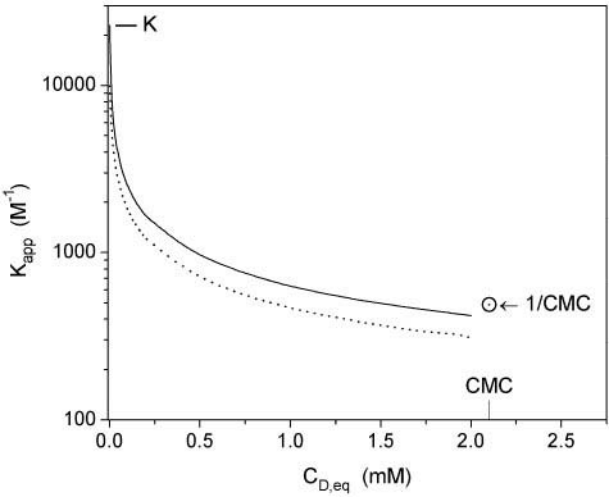

FIGURE 7 Variation of the apparent binding constant $K_{app} = Ke^{-\psi_0 F_0/RT}$ as a function of the SDS equilibrium constant for a noncharged POPC membrane. (—) $K = 2.3 \times 10^4\ M^{-1}$. (· · ·) $K = 1.0 \times 10^4\ M^{-1}$.

of −9 kcal/mol and varies only little with temperature. The main contribution to ΔG_D^0 comes from the enthalpy term (~60–70%) and SDS partitioning into lipid membranes is thus an enthalpy-driven reaction. In contrast, nonionic detergents partition into lipid bilayers because of a large gain in entropy.

The membrane partition constants of nonionic detergents have recently been summarized (Heerklotz and Seelig, 2000a; Table 1). In Fig. 5 *C* these data are translated into free energies, ΔG_D^0, and are plotted against the hydrocarbon chain length (□, nonionic detergents). The solid line represents the regression analysis. Also included in Fig. 5 *C* is the SDS partition constant (○), which fits well on the regression line. The slope of the straight line is −0.85 kcal/mol and yields the free energy per CH_2 group for the transfer from water into the bilayer membrane. An incremental change of ~−0.8 to −0.9 kcal/mol is typical for the transfer of hydrocarbons from water to a pure hydrocarbon phase or from water to the interior of micelles (Tanford, 1980). The ordered structure of the lipid bilayer thus appears to have little influence on the free energy of transfer.

Inspection of Table 1 reveals only small differences in the thermodynamic parameters of SDS for the various systems investigated. ΔH_D^0 is more exothermic and *K* is larger for SUVs compared with LUVs. This may be traced back to the looser lipid packing of the former, allowing easier SDS penetration (Beschiaschvili and Seelig, 1992). The SDS thermodynamic parameters for negatively charged POPC/POPG membrane are almost identical to those of neutral POPC bilayers. Again, this similarity is only discovered after correcting for electrostatic effects. In an actual titration experiment, the ITC curves clearly show less SDS binding to POPC/POPG membrane than to pure POPC vesicles due to increased electrostatic repulsion. LiDS exhibits the same binding parameters as SDS because it is the DS^- anion that determines the interaction with the membrane.

For most membrane biochemists the Gouy-Chapman theory is not readily available and binding is expressed in terms of an overall binding constant, K_{app}. For practical applications Fig. 7 hence displays the variation of $K_{app} = K e^{-z\psi_0 F_0/RT}$ as a function of the equilibrium SDS concentration. If the lipid vesicles are mixed with a sufficient excess of a given SDS concentration, the initial SDS concentration will also be the equilibrium concentration and the extent of SDS binding can be calculated according to $R_b = K_{app} \times C_D^0$. Theoretical curves for K_{app} are shown for 28°C with $K = 2.3 \times 10^4\ M^{-1}$ and 56°C with $K = 10^4\ M^{-1}$. At zero SDS concentration the K_{app}-values start at the theoretical *K* values. A sharp drop of K_{app} by approximately a factor of 10 occurs within the first interval of 0.2 mM SDS followed by a slower but continuous decrease in the higher concentration range. Eq. 10 predicts that the membrane is saturated with SDS at $R_b^{sat} = 0.28 \pm 0.04$ and $C_D^{sat} = 2.20\ mM \pm 0.60\ mM$.

Concluding remarks

It may be found surprising that no systematic thermodynamic studies on SDS partitioning into membranes have been available despite the widespread use of this detergent in membrane biochemistry. A number of reasons can be listed. First, to dissociate membranes SDS is usually used at high concentrations, concentrations well above the CMC. Knowledge of the SDS monomer-micelle phase diagram as a function of salt and temperature appears to be sufficient for this application (Becker et al., 1975). Second, SDS is difficult to measure. The molecule has no spectroscopic marker, and radioactive labeling is required for a direct measurement. Here isothermal titration calorimetry has an obvious advantage as the SDS interaction with the membrane leads to a considerable heat release. Third, the binding of SDS to the membrane occurs in two steps with apparently quite different time constants (at room temperature and low SDS concentrations). An initial fast binding (second) to the membrane outside is followed by a slow translocation (hours-days) to the inner half-layer (Kragh-Hansen et al., 1998; Lopez et al., 1998). Different binding results may thus be obtained depending on the time course of the experiment. In contrast, the ITC experiment is finished within 60 to 90 min, and a consistent interpretation of all ITC experiments at ambient temperatures was achieved by assuming a partitioning into the outer half-layer only. Finally, the analysis of partition data in any type of SDS binding experiment is made difficult by the superposition of electrostatic and hydrophobic contributions to the partition equilibrium. As the extent of DS^- in the membrane increases, so does the repulsive membrane potential, and the apparent binding constant varies according to the experimental conditions. This may explain the discrepancy between the partition constants available in the literature because they refer to

different experimental conditions. The present analysis demonstrates that a consistent interpretation of many different SDS partition experiments can be achieved with a single partition constant if electrostatic and hydrophobic effects are separated and properly accounted for. The SDS-POPC phase diagram at high water content could be established for SDS concentrations up to $C_D^0 \approx 12.5$ mM. The bilayer is disrupted at low concentrations of SDS in the membrane at $R_b^{sat} \sim 0.3$ and is completely solubilized at $R_b^{sol} \sim 2.2$. The spread between the first pertubation of the bilayer structure and its final solubilization is particularly large for this surfactant.

This work was supported by the Swiss National Science Foundation Grant 31-58800.99.

REFERENCES

Almog, S., B. J. Litman, W. Wimley, J. Cohen, E. J. Wachtel, Y. Barenholz, A. Ben-Shaul, and D. Lichtenberg. 1990. States of aggregation and phase transformations in mixtures of phosphatidylcholine and octyl glucoside. *Biochemistry.* 29:4582–4592.

Altenbach, C., and J. Seelig. 1984. Ca^{2+} binding to phosphatidylcholine bilayers as studied by deuterium magnetic resonance: evidence for the formation of a Ca^{2+} complex with two phospholipid molecules. *Biochemistry.* 23:3913–3920.

Aveyard, R., and D. A. Haydon. 1973. An introduction to the principles of surface chemistry. Cambridge University Press, London.

Becker, R., A. Helenius, and K. Simons. 1975. Solubilization of the Semliki Forest virus membrane with sodium dodecyl sulfate. *Biochemistry.* 14:1835–1841.

Beschiaschvili, G., and J. Seelig. 1992. Peptide binding to lipid bilayers: nonclassical hydrophobic effect and membrane-induced pK shifts. *Biochemistry.* 31:10044–10053.

Cantor, C. R., and P. R. Schimmel. 1980. Biophysical Chemistry. Freeman, San Francisco, CA.

Chatterjee, A., S. P. Moulik, S. K. Sanyal, B. K. Mishra, and P. M. Puri. 2001. Thermodynamics of micelle formation of ionic surfactants: a critical assessment for sodium dodecyl sulfate, cetyl pyridinium chloride and dioctyl sulfosuccinate (Na Salt) by microcalorimetric, conductometric, and tensiometric measurements. *J. Phys. Chem. B.* 105: 12823–12831.

Cocera, M., O. Lopez, J. Estelrich, J. L. Parra, and A. de la Maza. 1999. Transbilayer movement of sodium dodecyl sulfate in large unilamellar phospholid vesicles. *Langmuir.* 15:6609–6612.

Cocera, M., O. López, J. Estelrich, J. L. Parra, and A. de la Maza. 2000. Kinetic and structural aspects of the adsorption of sodium dodecyl sulfate on phosphatidylcholine liposomes. *Langmuir.* 16:4068–4071.

Cocera, M., O. Lopez, J. Estelrich, J. L. Parra, and A. de la Maza. 2001. Use of a fluorescence spectroscopy technique to study the adsorption of sodium dodecylsulfonate on liposomes. *Chem. Phys. Lipids.* 110:19–26.

Gazzara, J. A., M. C. Phillips, S. Lund-Katz, M. N. Palgunachari, J. P. Segrest, G. M. Anantharamaiah, W. V. Rodrigueza, and J. W. Snow. 1997. Effect of vesicle size on their interaction with class A amphipathic helical peptides. *J. Lipid Res.* 38:2147–2154.

Heerklotz, H., and J. Seelig. 2000a. Correlation of membrane/water partition coefficients of detergents with the critical micelle concentration. *Biophys. J.* 78:2435–2440.

Heerklotz, H., and J. Seelig. 2000b. Titration calorimetry of surfactant-membrane partitioning and membrane solubilization. *Biochim. Biophys. Acta.* 1508:69–85.

Kragh-Hansen, U., M. le Maire, and J. V. Møller. 1998. The mechanism of detergent solubilization of liposomes and protein-containing membranes. *Biophys. J.* 75:2932–2946.

Lasch, J. 1995. Interaction of detergents with lipid vesicles. *Biochim. Biophys. Acta.* 1241:269–292.

Lichtenberg, D., R. J. Robson, and E. A. Dennis. 1983. Solubilization of phospholipids by detergents: structural and kinetic aspects. *Biochim. Biophys. Acta.* 737:285–304.

Lopez, O., M. Cocera, R. Pons, N. Azemar, and A. de la Maza. 1998. Kinetic studies of liposome solubilization by sodium dodecyl sulfate based on a dynamic light scattering technique. *Langmuir.* 14: 4671–4674.

Lopez, O., M. Cocera, E. Wehrli, J. L. Parra, and A. de la Maza. 1999. Solubilization of liposomes by sodium dodecyl sulfate: new mechanism based on the direct formation of mixed micelles. *Arch. Biochem. Biophys.* 367:153–160.

MacDonald, R. C., R. I. MacDonald, B. P. Menco, K. Takeshita, N. K. Subbarao, and L. R. Hu. 1991. Small-volume extrusion apparatus for preparation of large, unilamellar vesicles. *Biochim. Biophys. Acta.* 1061: 297–303.

Majhi, P. R., and A. Blume. 2001. Thermodynamic characterization of temperature-induced micellization and demicellization of detergents studied by differential scanning calorimetry. *Langmuir.* 17:3844–3851.

McLaughlin, S. 1977. Electrostatic potentials at membrane-solution interfaces. *Curr. Top. Membr. Transp.* 9:71–144.

Mysels, K. J., and L. H. Princen. 1959. Light scattering by some lauryl sulfate solutions. *J. Phys. Chem.* 63:1696–1700.

Nebel, S., P. Ganz, and J. Seelig. 1997. Heat changes in lipid membranes under sudden osmotic stress. *Biochemistry.* 36:2853–2859.

Paula, S., W. Süs, J. Tuchtenhagen, and A. Blume. 1995. Thermodynamis of micelle formation as a function of temperature: a high sensitivity titration calorimetry study. *J. Phys. Chem.* 99:11742–11751.

Richieri, G. V., R. T. Ogata, and A. M. Kleinfeld. 1995. Thermodynamics of fatty acid binding to fatty acid-binding proteins and fatty acid partition between water and membranes measured using the fluorescent probe ADIFAB. *J. Biol. Chem.* 270:15076–15084.

Schurtenberger, P., N. Mazer, and W. Kanzig. 1985. Micelle to vesicle transition in aqueous-solutions of bile-salt and lecithin. *J. Phys. Chem.* 89:1042–1049.

Tanford, C. 1980. The Hydrophobic Effect: Formation of Micelles and Biological Membranes. Wiley, New York.

Wenk, M. R., T. Alt, A. Seelig, and J. Seelig. 1997. Octyl-β-D-glucopyranoside partitioning into lipid bilayers: thermodynamics of binding and structural changes of the bilayer. *Biophys. J.* 72:1719–1731.

Wenk, M. R., and J. Seelig. 1997. Interaction of octyl-beta-thioglucopyranoside with lipid membranes. *Biophys. J.* 73:2565–2574.

Wiseman, T., S. Williston, J. F. Brandts, and L. N. Lin. 1989. Rapid measurement of binding constants and heats of binding using a new titration calorimeter. *Anal. Biochem.* 179:131–137.